

Experimental validation of positioning and tracking system using ultra-wideband and low-cost microcontroller units

Ngoc-Son Duong, Minh-Tuyen Vu, Minh-Duc Nguyen, Thai-Mai Dinh Thi

Department of Telecommunications Systems, Faculty of Electronics and Telecommunications, VNU University of Engineering and Technology, Hanoi, Vietnam

Article Info

Article history:

Received Oct 22, 2024

Revised Jun 30, 2025

Accepted Aug 1, 2025

Keywords:

Arduino Uno R3

DW1000

ESP8266

Indoor positioning systems

Ultra-wideband

ABSTRACT

Indoor positioning systems (IPS) have become increasingly critical in various applications, from asset tracking to smart environments. While global positioning system (GPS) offers precise outdoor localization, its signal is unavailable indoors. Ultra-wideband (UWB) technology emerges as a promising alternative due to its high accuracy, robustness against multipath interference, and ability to operate in dense environments. Aiming to develop an affordable and efficient system, we present a UWB-based IPS using the DW1000 UWB chip, evaluated with two different low-cost microcontroller units (MCUs): the ESP8266 system-on-chip (SoC) and the Arduino Uno R3. The findings suggest that the ESP8266 SoC is a superior choice for building an affordable and efficient UWB IPS, making it a compelling option for widespread adoption in budget-sensitive applications.

This is an open access article under the [CC BY-SA](#) license.



Corresponding Author:

Thai-Mai Dinh Thi

Department of Telecommunications Systems, Faculty of Electronics and Telecommunications

VNU University of Engineering and Technology

Hanoi 100000, Vietnam

Email: dttmai@vnu.edu.vn

1. INTRODUCTION

In an increasingly connected world, the demand for accurate indoor positioning systems (IPS) has surged [1]. The traditional global navigation satellite system (GNSS), while highly effective outdoors, falls short within enclosed environments. GNSS signals struggle to penetrate walls and other structures, leading to diminished accuracy and reliability indoors. This limitation underscores the importance of developing robust indoor positioning solutions, especially as the need for precise location tracking expands across various sectors. Indoor positioning systems have become essential in a wide range of applications. In retail and marketing, they enable businesses to deliver personalized content and promotions to customers based on their location within a store. In the gaming industry, IPS facilitates augmented reality experiences, allowing players to interact with virtual elements seamlessly integrated into physical spaces. Smart environments, including homes and offices, leverage indoor positioning to enhance automation and energy efficiency by tracking the location of occupants. These examples illustrate the broad and growing significance of accurate indoor positioning in modern technology landscapes. Among the various technologies employed in IPS, ultra-wideband (UWB) [2], [3] stands out for its unique advantages. Unlike wireless fidelity (Wi-Fi) [4], Bluetooth low energy (BLE) [5], and radio-frequency identification [6] or radar [7], UWB offers superior accuracy, often within centimeters, due to its high time resolution and ability to operate over a wide frequency spectrum. This makes UWB particularly well-suited for environments where precision is critical. Furthermore, UWB's low susceptibility to interference and multipath effects [8], which are common challenges in indoor environments, enhances its reliability compared to other technologies [9].

The limitations of GNSS for indoor positioning have led to investigations by many organizations and scientists in finding alternatives. Among many technologies, UWB is most suitable for indoor positioning due to its high accuracy, resistance to multipath interference, and ability to function well in non-line-of-sight (NLOS) conditions, making it ideal for complex indoor environments. Jiang *et al.* [10] consider a UWB-based positioning system for outdoor-indoor transition zones. In this study, a tightly coupled GNSS/UWB/inertial navigation system (INS) integration system is proposed. For indoor use, UWB helps correct INS errors to achieve centimeter-level accuracy. In GNSS-challenged areas, the system ensures continuous, accurate positioning. An experiment in a high-rise building showed the system's effectiveness, achieving a mean square error of 10.18 cm, providing seamless indoor-outdoor positioning. Liu *et al.* [11] introduce a novel method called dynamic feasible region-based particle filtering to improve the accuracy and stability of UWB indoor positioning. It addresses the challenges of particle convergence for particle filter in NLOS conditions by dynamically adjusting the observation likelihood function based on signal power quality. Experimental results demonstrate the effectiveness of the proposed method in complex indoor environments. Indoor positioning systems using UWB can be used not only for humans but also for robots. Zhu *et al.* [12] introduce a novel method for building an error map for UWB indoor positioning, which can help improve the accuracy of the mobile robot system. The method adapts the distribution of measurement points to a rough error distribution and uses the error map in a particle filter to improve positioning accuracy. The results show a significant reduction in the number of measurement points required and better positioning accuracy with faster convergence speed. Wang *et al.* [13], present a novel method for UWB-based IPS that addresses the challenges of NLOS interference. The method utilizes a prior environmental map to identify line-of-sight (LOS) and NLOS anchors and then corrects NLOS observations. A map-modified Kalman filtering algorithm is used to optimize the trajectory. The experimental results show that the proposed method significantly improves positioning accuracy compared to traditional filtering algorithms, especially in NLOS environments with few anchors. Meanwhile, Feng *et al.* [14] introduce an integrated IPS combining inertial navigation system (INS) and UWB to improve accuracy and robustness. It discusses the relationship between the base station's distribution and dilution of precision, and uses extended Kalman filter and unscented Kalman filter (UKF) for fusion. Simulation results show that the proposed IPS has a higher accuracy compared to the one that only uses UWB with least square estimation. The problems of antenna calibration for UWB-based IPS are currently considered in [15]. In this study, the authors present a novel calibration and compensation algorithm for UWB-based ranging. It addresses the limitations of existing methods by considering second-order error terms and distance constraints between anchors. By integrating UWB and built-in sensor measurements, the algorithm estimates target positions using dual UKF and UWB ranging. Experimental results demonstrate the effectiveness of the proposed method in achieving high-precision calibration with an error of approximately 6 cm. Real-world applications of UWB-based positioning can be found in [16], [17].

Despite these advantages, the deployment of UWB technology on low-cost microcontroller units (MCUs) remains underexplored. While most research has focused on UWB implementation using high-performance, often costly, hardware, the potential for integrating UWB with affordable MCUs is significant, especially for applications requiring large-scale deployment or cost-sensitive environments. This paper aims to fill this gap by experimentally validating an indoor positioning system that utilizes UWB technology in conjunction with a low-cost MCU, offering a scalable and cost-effective solution for high-precision indoor localization.

2. THE PROPOSED SYSTEM

The architecture of the proposed system is depicted in Figure 1. Our system can be divided into two main parts: positioning and tracking. The positioning part consists of UWB DW1000 [18] chips connected to microcontrollers. They consist of multiple anchors and a tag. In the positioning part, the locations of the anchors are considered to be known in advance. The task of the system is to determine the unknown location of the tag when the signals of nearby anchors are available. By exchanging UWB packets, the tag extracts information about the time of arrival (TOA) between it and multiple anchors and calculates the distance. When the tag has collected the distance to at least 3 anchors, the microcontroller then calculates the location of the tag through the least square method. The returned locations are multiple points and tend to be unstable. Therefore, a Kalman filter [19] is added to stabilize them. The tracking part consists of a server and a control monitor. It has the function of receiving information from the positioning part and displaying the location information of the tag to the subscribers. The connection between these blocks is the message queue telemetry transport protocol (MQTT) [20]. MQTT herein is a protocol for message transmission based on the publish/subscribe model. It relies on a broker (intermediary point) and is designed to be open, not tied to any specific application, very simple, and easy to integrate, especially due to its fast processing speed. It is particularly well-suited for Internet of Thing models. For the proposed IPS, which are typically local systems in a fixed space, MQTT ensures low

latency in the tracking process. Moreover, for hardware-based systems with limited resources such as memory or processing speed, MQTT is one of the optimal choices.

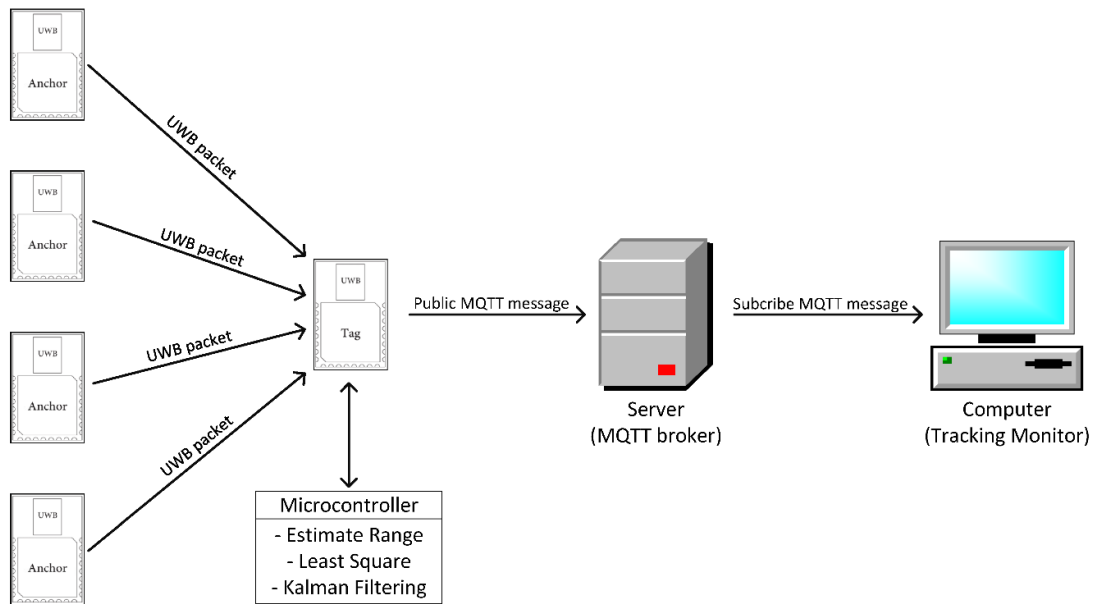


Figure 1. Architecture of proposed UWB-based indoor positioning system

3. METHOD

3.1. Single-sided two-way ranging (SS-TWR)

SS-TWR involves a straightforward measurement of the round-trip time (RTT) of a single message sent from one node to another, followed by a response sent back to the original node. The operation of SS-TWR is illustrated in Figure 2, where a tag starts the exchange and an anchor responds to complete it. In order to calculate the time of flight (ToF), each device will record its timestamp and attach it to the message whenever it is sending or receiving. Based on Figure 2, the mathematical representation of ToF, denoted by τ , would be:

$$\tau = \frac{1}{2}(T_{R1} - D_1) \quad (1)$$

where T_{R1} and D_1 are RTT and processing time (or delay time) of the anchor, respectively. Because each device has their own local clock, each ToF is independently measured and therefore contains their clock offset error.

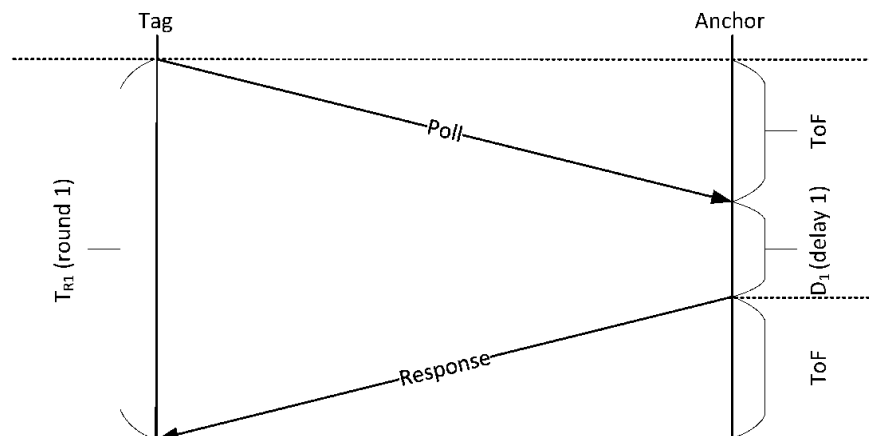


Figure 2. Single-sided two-way ranging protocol

3.2. Symmetric double-sided two-ways ranging (SDS-TWR)

SDS-TWR is a method that requires both devices to have synchronized clocks and uses a sequence of messages exchanged between the two devices. The first message is sent from the initiator (tag) to the responder (anchor), and the anchor sends a response message back to the tag. The timestamps of these messages are used to calculate the RTT and therefore the distance between the two devices. At the beginning, the tag device will send a probing packet (a poll) to neighboring devices. When nearby anchor devices receive the packet, they will respond back to the tag with a packet with another timestamp. When the tag device receives the response packet from the anchor, it will record the time of reception response and compose the final notification to send. Based on recorded timestamps, anchor can determine the ToF and hence the distance between it and the tag. The procedure of the SDS-TWR protocol is illustrated by Figure 3. As shown in Figure 3, we have:

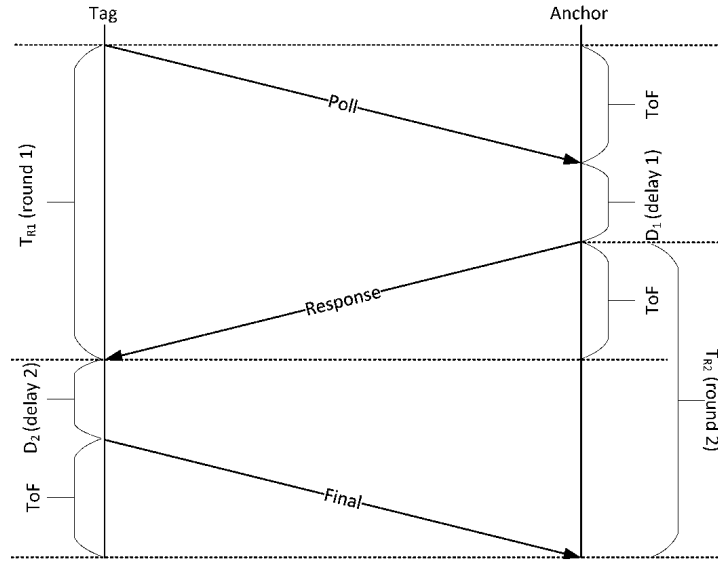


Figure 3. Double-sided two-way ranging protocol

$$T_{R_1} = 2\tau + D_1 \quad (2)$$

$$T_{R_2} = 2\tau + D_2 \quad (3)$$

This is equivalent to (4).

$$\tau = \frac{T_{R_1} - D_2 + T_{R_2} - D_1}{4} \quad (4)$$

Taking into account the clock drift error, say ϵ_A and ϵ_B , affecting measurements, i.e., $\hat{T}_{R_1} = (1 + \epsilon_A)T_{R_1} = k_1 T_{R_1}$, $\hat{T}_{R_2} = (1 + \epsilon_B)T_{R_2} = k_2 T_{R_2}$, $\hat{D}_2 = (1 + \epsilon_A)D_2 = k_1 D_2$, and $\hat{D}_1 = (1 + \epsilon_B)D_1 = k_2 D_1$, the estimated ToF is:

$$\hat{\tau} = \frac{\hat{T}_{R_1} - \hat{D}_2 + \hat{T}_{R_2} - \hat{D}_1}{4} \quad (5)$$

The error between estimated and exact ToF is then (6):

$$\hat{\tau} - \tau = \frac{\epsilon_A(T_{R_1} - D_2) + \epsilon_B(T_{R_2} - D_1)}{4} \quad (6)$$

Replacing T_{R_1} and T_{R_2} with (2) and (3), respectively, we finally have (7):

$$\hat{\tau} - \tau = \frac{1}{2}\tau(\epsilon_A + \epsilon_B) + \frac{1}{4}(\epsilon_A - \epsilon_B)(D_1 - D_2) \quad (7)$$

3.3. Asymmetric double-sided two-way ranging (ADS-TWR)

The timestamp exchange for ADS-TWR is the same as SDS-TWR, but the mathematical manipulation is different [21]. Starting by multiplying (2) and (3), we have:

$$T_{R_1}T_{R_2} = (2\tau + D_1)(2\tau + D_2) \quad (8)$$

This is equivalent to (9):

$$T_{R_1}T_{R_2} - D_2D_1 = 2\tau(2\tau + D_1 + D_2) \quad (9)$$

Then, we obtain:

$$T_{R_1}T_{R_2} - D_2D_1 = 2\tau(T_{R_1} + D_2) \quad (10)$$

$$T_{R_1}T_{R_2} - D_2D_1 = 2\tau(T_{R_2} + D_1) \quad (11)$$

From (2) and (3), they imply that $(T_{R_1} + D_2) = (T_{R_2} + D_1)$ which can be used to rewrite as (12):

$$\tau = \frac{T_{R_1}T_{R_2} - D_2D_1}{T_{R_1} + D_2 + T_{R_2} + D_1} \quad (12)$$

Considering clock drift, the estimated ToF is modeled as (13):

$$\hat{\tau} = \frac{\hat{T}_{R_1}\hat{T}_{R_2} - \hat{D}_2\hat{D}_1}{\hat{T}_{R_1} + \hat{D}_2 + \hat{T}_{R_2} + \hat{D}_1} \quad (13)$$

Similar to the SDS-TWR, we have (14) and (15):

$$\hat{\tau} = \frac{k_1k_2}{k_2} \frac{T_{R_1}T_{R_2} - D_2D_1}{2(T_{R_1} + D_2)} \quad (14)$$

$$\hat{\tau} = \frac{k_1k_2}{k_2} \frac{T_{R_1}T_{R_2} - D_2D_1}{2(T_{R_2} + D_1)} \quad (15)$$

Finally, the error between estimated ToF and exact ToF can be calculated as (16) and (17).

$$\hat{\tau} - \tau = k_1\tau - \tau = \epsilon_A\tau \quad (16)$$

$$\hat{\tau} - \tau = k_2\tau - \tau = \epsilon_B\tau \quad (17)$$

3.4. Positioning algorithm

Assuming there are N anchors and a tag with coordinates $[x_i, y_i]^T, (i \in \{1, \dots, N\})$ and $[x, y]^T$ respectively. The Euclidean distance between the i -th anchor and the tag can be written as (18):

$$d_i = \sqrt{(x - x_i)^2 + (y - y_i)^2} \quad (18)$$

As shown in (18) can be written as (19):

$$\begin{cases} d_1^2 = (x - x_1)^2 + (y - y_1)^2 \\ d_2^2 = (x - x_2)^2 + (y - y_2)^2 \\ \vdots \\ d_n^2 = (x - x_n)^2 + (y - y_n)^2 \end{cases} \quad (19)$$

The matrix form of the above system can be written as (20):

$$Ax_{LS} = b \quad (20)$$

where:

$$A = \begin{bmatrix} x_2 - x_1 & y_2 - y_1 \\ x_3 - x_1 & y_3 - y_1 \\ \dots & \dots \\ x_N - x_1 & y_N - y_1 \end{bmatrix}, b = \frac{1}{2} \begin{bmatrix} x_2^2 + y_2^2 - d_2^2 - (x_1^2 + y_1^2 - d_1^2) \\ x_3^2 + y_3^2 - d_3^2 - (x_1^2 + y_1^2 - d_1^2) \\ \dots \\ x_N^2 + y_N^2 - d_N^2 - (x_1^2 + y_1^2 - d_1^2) \end{bmatrix}, \text{ and } x_{LS} = \begin{bmatrix} x_{LS} \\ y_{LS} \end{bmatrix}$$

The optimal solution for x_{LS} is [22].

$$x_{LS} = (A^T A)^{-1} A^T b \quad (21)$$

3.5. Stabilization

Considering a system with a position-velocity model [23] in two-dimensional where the velocities along the axis (x, y) are denoted by (\dot{x}, \dot{y}) . The system state at time step k can be written as:

$$x_k = [x, y, \dot{x}, \dot{y}]^T \quad (22)$$

At the beginning, the previous position, x_{k-1} , is propagated to the current time step k in the prediction step as:

$$\hat{x}_{k|k-1} = F \hat{x}_{k-1} \quad (23)$$

where F is the transition matrix and can be defined by:

$$F = \begin{bmatrix} 1 & 0 & \Delta t & 0 \\ 0 & 1 & 0 & \Delta t \\ 0 & 0 & 1 & 0 \\ 0 & 0 & 0 & 1 \end{bmatrix} \quad (24)$$

Let $\hat{P}_{k-1|k-1}$ be the posterior covariance matrix of \hat{x} at time step $k-1$, say \hat{x}_{k-1} , then the prior covariance matrix $\hat{P}_{k|k-1}$ of \hat{x}_{k-1} is determined by (25):

$$P_{k|k-1} = F_k P_{k-1|k-1} F_k^T + Q \quad (25)$$

where Q is the covariance matrix of the process noise. In the correction step, the prior state vector is corrected based on the measurement z . The vector y describes the difference between the measurement z and the measurement model $h(x)$ applied to the predicted state as (26):

$$y = z - h(\hat{x}_{k|k-1}) \quad (26)$$

The measuring model is modeled as (27).

$$h(\hat{x}) = d_i = \sqrt{(x - x_i)^2 + (y - y_i)^2} \quad (27)$$

After a new range is obtained, the prediction is made as (28):

$$\hat{x}_{k|k} = \hat{x}_{k|k-1} + K_k y_k \quad (28)$$

Herein, the measurement's degree of confidence in relation to the prediction is expressed as a Kalman gain, denoted by K . With R standing for measurement noise covariance matrix, Kalman gain is calculated as (29):

$$K_k = \hat{P}_{k|k-1} H_k^T (H_k \hat{P}_{k|k-1} H_k^T + R)^{-1} \quad (29)$$

where H is calculated as (30):

$$H_k = \left(\frac{\partial h(\hat{x}_k)}{\partial x}, \frac{\partial h(\hat{x}_k)}{\partial y}, 0, 0 \right) \quad (30)$$

Finally, the posterior covariance matrix is calculated as (31):

$$\hat{P}_{k|k} = (I - K_k H_k) \hat{P}_{k|k-1} \quad (31)$$

4. RESULTS AND DISCUSSION

4.1. Experimental setup

In the experiment, we chose to use the DW1000 UWB module as the main positioning chip due to its advantages, such as precise ranging and localization capabilities. To localize a single tag, we place 4 anchors at a height of approximately 80 cm around an interested area. The experimental setup is shown in Figure 4. The user will carry the tag with them so we can track their movements. The modules will each be paired with an ESP8266 microcontroller [24] or an Arduino Uno R3 microcontroller [25] to run the algorithms. The experiment on the two microcontrollers was carried out separately with each system use distinctively one of the two microcontrollers. A Wi-Fi base station will be used to receive their respective data and transmit it using to a computer using MQTT where the final calculations are made to determine the location of the user at the experiment site. It's to be noted that in the case of the experiment with the Arduino Uno, an ESP8266 is implemented but not being used to process data but only to send and receive data using Wi-Fi, the main processing unit in this case is still the ATmega328p that came default with the Arduino. Experiments were conducted in a lab environment of approximately 3 m by 16.8 m. In this environment, the signal is altered and quite noisy due to the activities of pedestrians, but at the same time, it is also a way to realistically assess the accuracy of the proposed system in a real environment. The experiment involved the user walking in a predetermined pattern to compare the real-time tracking to the planned path. The return data is in the form of coordinate related to the testing area. The data from the Tag device will then be send via a closed Wi-Fi network to keep low system latency and be collected by a computer that have the tracking software installed where the path of the user can be draw according to the data. For the Kalman filter, we observed that the error of the UWB sensor is about 15 cm, so the entries on the main diagonal of Q are set to $[0.15]^2$ and the other entries are set to 0.

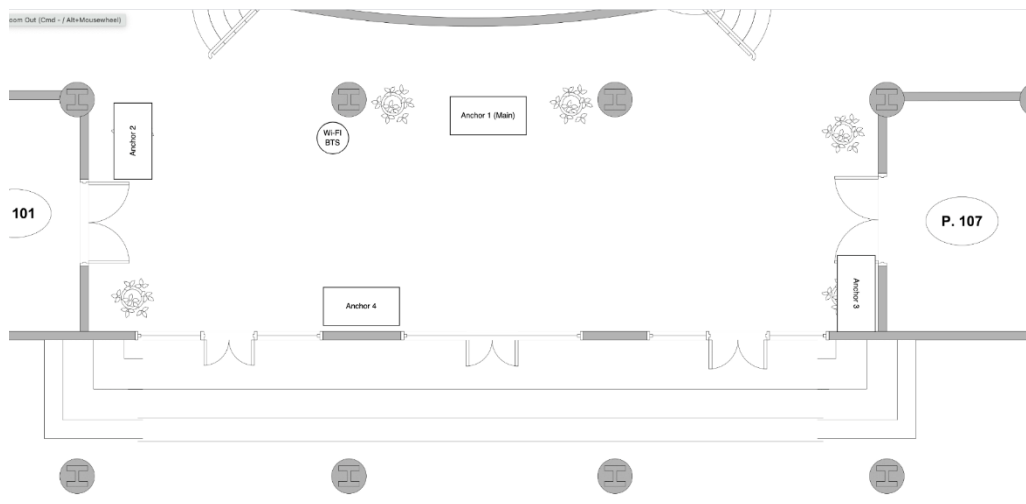


Figure 4. Experimental system setup

3.2. Results and discussion

3.2.1. On the performance of double-sided ranging methods

In the first experiment, we want to assert which ranging method should be used for an indoor positioning system. Figure 5 shows the performance of the two mentioned ranging schemes. Both protocols were conducted in the same environment. As can be seen in Figure 5, the accuracy of ADS-TWR is higher than SDS-TWR at any distance. This happens because the delay on sender and responder is different, i.e., $D_1 \neq D_2$. Hence, this introduces an extra term $\frac{1}{4}(\epsilon_A - \epsilon_B)(D_1 - D_2)$ for (7). Meanwhile, the analytical error of ADS-TWR in (16) and (17) does not depend on the delay of any device. Once the clock drift is carefully calibrated, the error of ADS-TWR will always be smaller than SDS-TWR. In this experiment, detailed statistics show that the average errors of ADS-TWR and SDS-TWR are 0.12 m and 0.22 m, respectively.

3.2.2. On the accuracy of the proposed system with 2 low-cost MCUs

The tracking results of the ESP8266-based system are shown in Figure 6. In Figure 6, the red dots, black line, and blue line represent the positions returned by the localization algorithm, the estimated path stabilized by the Kalman algorithm, and the actual path, respectively. As we can see, it shows that the system

can track the user with high accuracy as the pattern of the estimated path compared to the exact path. The effect of multipath can be observed, as returned positions are either scattered or oscillate in the distance measurement, this effect is filtered out by the Kalman filter. In addition, we can positioning algorithm. The usage of Kalman filter also filtered out the effects of multipath, as evidenced by the result in Figure 6. The error statistics of the ESP8266-based and Arduino-based positioning systems are given in Figure 7. As can be seen, the errors of both systems are relatively good, say, 99 % with errors below 1 m. It is noteworthy that the accuracy of the positioning system on ESP8266 is better than the positioning system on Arduino. The average errors of the positioning system on the ESP8266 and on the Arduino are 0.25 m and 0.4 m, respectively. This happens because the ESP8266 has a better memory and processing power, which helps it process complex algorithms with large data streams in a shorter time. This helps reducing the latency of the system significantly. We determine that by assigning a timestamp to each result printed then measuring the result rate of the system in times per second. In this experiment, we observe that the update rate of Arduino is at about 3 times per second, whereas on the ESP8266, the update rate is 6 times per second. This phenomenon can be explained by the fact that the ESP8266 has a higher clock speed than the Arduino (16 MHz vs 160 MHz) and larger memory (2 Kb vs 128 Kb). The antenna delay is also eliminated by calibration before the experiment. Therefore, we determine that the system is capable of tracking objects in real-time.

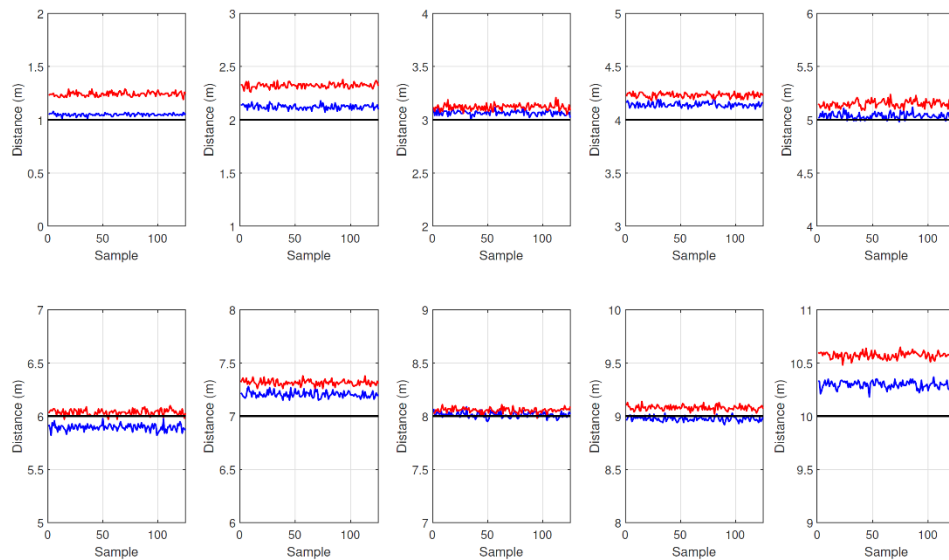


Figure 5. Experimental results of ADS-TWR and SDS-TWR from 1 to 10 m. Legend: Black, blue and red lines denote exact range, range from ADS-TWR and range from SDS-TWR, respectively

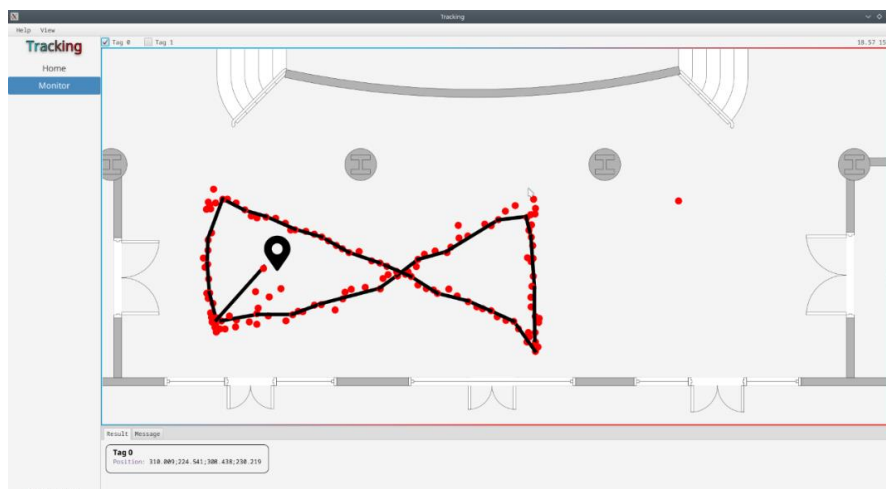


Figure 6. Tracking results of ESP8266-based system

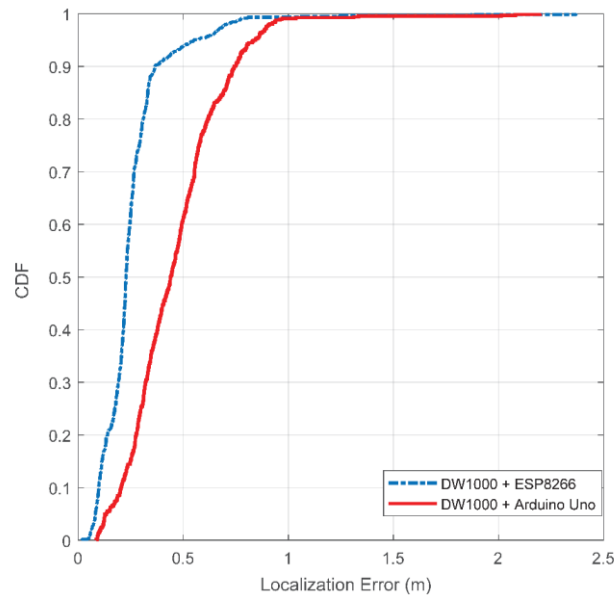


Figure 7. Comparison of localization error between Arduino-based and ESP8266-based UWB positioning system

5. CONCLUSION

In this study, we have compared the indoor positioning system using UWB on two low-cost microprocessor platforms, including ESP8266 and Arduino. The results show that the positioning system has better accuracy when it uses ESP8266 and ADS-TWR distance estimation. This result promotes the commercialization of indoor positioning systems, especially low-cost systems based on UWB. Despite these achievements, several limitations must be acknowledged. First, the experiments were conducted in a controlled lab environment with limited dimensions, which may not fully capture the challenges of larger or more diverse real-world scenarios. Second, our system assumes anchor positions are predetermined, which may not always be feasible or accurate in dynamic or ad-hoc deployment scenarios. In addition to the achieved results, the research can further develop in some directions, including: incorporating additional devices, including mobile devices with UWB sensor, considering better energy efficiency and compatibility by incorporating BLE as an additional source of data for positioning and system performance in NLOS situations.

FUNDING INFORMATION

No funding was involved.

AUTHOR CONTRIBUTIONS STATEMENT

This journal uses the Contributor Roles Taxonomy (CRediT) to recognize individual author contributions, reduce authorship disputes, and facilitate collaboration.

Name of Author	C	M	So	Va	Fo	I	R	D	O	E	Vi	Su	P	Fu
Ngoc-Son Duong	✓	✓		✓	✓	✓	✓			✓	✓			
Minh-Tuyen Vu	✓		✓		✓			✓	✓	✓	✓			
Minh-Duc Nguyen			✓			✓		✓		✓				
Thai-Mai Dinh Thi	✓	✓		✓		✓	✓			✓		✓	✓	

C : **C**onceptualization

M : **M**ethodology

So : **S**oftware

Va : **V**alidation

Fo : **F**ormal analysis

I : **I**nterpretation

R : **R**esources

D : **D**ata Curation

O : **O**riginal Draft

E : **E**diting

Vi : **V**isualization

Su : **S**upervision

P : **P**roject administration

Fu : **F**unding acquisition

CONFLICT OF INTEREST STATEMENT

The authors declare that they have no conflict of interest.

DATA AVAILABILITY




Data availability is not applicable to this paper.

REFERENCES




- [1] P. S. Farahsari, A. Farahzadi, J. Rezaadeh, and A. Bagheri, "A survey on indoor positioning systems for IoT-based applications," *IEEE Internet of Things Journal*, vol. 9, no. 10, pp. 7680–7699, May 2022, doi: 10.1109/JIOT.2022.3149048.
- [2] Y. Gao, O. Postolache, Y. Yang, and B. Yang, "UWB system and algorithms for indoor positioning," in *2021 Telecoms Conference (ConfTELE)*, Feb. 2021, pp. 1–6. doi: 10.1109/ConfTELE50222.2021.9435577.
- [3] C. L. Sang, M. Adams, M. Hesse, and U. Rückert, "Bidirectional UWB localization: A review on an elastic positioning scheme for GNSS-deprived zones," *IEEE Journal of Indoor and Seamless Positioning and Navigation*, vol. 1, pp. 161–179, 2023, doi: 10.1109/JISPIN.2023.3337055.
- [4] S. Li and X. Huang, "Indoor fingerprint positioning based on WiFi channel state information," in *2023 42nd Chinese Control Conference (CCC)*, Jul. 2023, pp. 3526–3531. doi: 10.23919/CCC58697.2023.10240200.
- [5] A. Handojo, T. Octavia, R. Lim, and J. K. Anggita, "Indoor positioning system using BLE beacon to improve knowledge about museum visitors," *TELKOMNIKA (Telecommunication Computing Electronics and Control)*, vol. 18, no. 2, pp. 792–798, Apr. 2020, doi: 10.12928/telkomnika.v18i2.14886.
- [6] A. Vena, I. Illanes, L. Alidieres, B. Sorli, and F. Perea, "RFID based indoor localization system to analyze visitor behavior in a Museum," in *2021 IEEE International Conference on RFID Technology and Applications (RFID-TA)*, Oct. 2021, pp. 183–186. doi: 10.1109/RFID-TA53372.2021.9617265.
- [7] A. Sesyuk, S. Ioannou, and M. Raspopoulos, "Radar-based millimeter-wave sensing for accurate 3-D indoor positioning: Potentials and challenges," *IEEE Journal of Indoor and Seamless Positioning and Navigation*, vol. 2, pp. 61–75, 2024, doi: 10.1109/JISPIN.2024.3359151.
- [8] V. Schejbal, D. Cermak, Z. Nemec, P. Bezousek, and O. Fiser, "Multipath propagation effects of UWB radars," in *2006 International Conference on Microwaves, Radar & Wireless Communications*, May 2006, pp. 1188–1191. doi: 10.1109/MIKON.2006.4345400.
- [9] J.-S. Lee, Y.-W. Su, and C.-C. Shen, "A comparative study of wireless protocols: Bluetooth, UWB, ZigBee, and Wi-Fi," in *IECON 2007 - 33rd Annual Conference of the IEEE Industrial Electronics Society*, 2007, pp. 46–51. doi: 10.1109/IECON.2007.4460126.
- [10] W. Jiang, Z. Cao, B. Cai, B. Li, and J. Wang, "Indoor and outdoor seamless positioning method using UWB enhanced multi-sensor tightly-coupled integration," *IEEE Transactions on Vehicular Technology*, vol. 70, no. 10, pp. 10633–10645, Oct. 2021, doi: 10.1109/TVT.2021.3110325.
- [11] J. Liu, L. Zhang, J. Xu, and J. Shi, "Dynamic feasible region-based IMU/UWB fusion method for indoor positioning," *IEEE Sensors Journal*, vol. 24, no. 13, pp. 21447–21457, Jul. 2024, doi: 10.1109/JSEN.2024.3398789.
- [12] X. Zhu, J. Yi, J. Cheng, and L. He, "Adapted error map based mobile robot UWB indoor positioning," *IEEE Transactions on Instrumentation and Measurement*, vol. 69, no. 9, pp. 6336–6350, Sep. 2020, doi: 10.1109/TIM.2020.2967114.
- [13] Q. Wang, Z. Li, H. Zhang, Y. Yang, and X. Meng, "An indoor UWB NLOS correction positioning method based on anchor LOS/NLOS map," *IEEE Sensors Journal*, vol. 23, no. 24, pp. 30739–30750, Dec. 2023, doi: 10.1109/JSEN.2023.3328715.
- [14] D. Feng, C. Wang, C. He, Y. Zhuang, and X.-G. Xia, "Kalman-filter-based integration of IMU and UWB for high-accuracy indoor positioning and navigation," *IEEE Internet of Things Journal*, vol. 7, no. 4, pp. 3133–3146, Apr. 2020, doi: 10.1109/JIOT.2020.2965115.
- [15] M. Qi, B. Xue, and W. Wang, "Calibration and compensation of anchor positions for UWB indoor localization," *IEEE Sensors Journal*, vol. 24, no. 1, pp. 689–699, Jan. 2024, doi: 10.1109/JSEN.2023.3329535.
- [16] A. Juárez, S. Fortes, E. Colin, C. Baena, E. Baena, and R. Barco, "UWB-based positioning system for indoor sports," in *2023 13th International Conference on Indoor Positioning and Indoor Navigation (IPIN)*, Sep. 2023, pp. 1–6. doi: 10.1109/IPIN57070.2023.10332477.
- [17] F. Geyer and D. Schupke, "Precise onboard aircraft cabin localization using UWB and ML," in *GLOBECOM 2022 - 2022 IEEE Global Communications Conference*, Dec. 2022, pp. 2032–2037. doi: 10.1109/GLOBECOM48099.2022.10000651.
- [18] J. Sidorenko, V. Schatz, N. Scherer-Negenborn, M. Arens, and U. Hugentobler, "Error corrections for ultrawideband ranging," *IEEE Transactions on Instrumentation and Measurement*, vol. 69, no. 11, pp. 9037–9047, Nov. 2020, doi: 10.1109/TIM.2020.2996706.
- [19] G. Welch and G. Bishop, "An introduction to the Kalman filter." TR 95-041 Department of Computer Science University of North Carolina at Chapel Hill Chapel Hill, pp. 1–16, 2006.
- [20] S. S. Prayogo, Y. Mukhlis, and B. K. Yakti, "The use and performance of MQTT and CoAP as internet of things application protocol using NodeMCU ESP8266," in *2019 Fourth International Conference on Informatics and Computing (ICIC)*, Oct. 2019, pp. 1–5. doi: 10.1109/ICIC47613.2019.8985850.
- [21] D. Neiryneck, E. Luk, and M. McLaughlin, "An alternative double-sided two-way ranging method," in *2016 13th Workshop on Positioning, Navigation and Communications (WPNC)*, Oct. 2016, pp. 1–4. doi: 10.1109/WPNC.2016.7822844.
- [22] T.-M. T. Dinh, N.-S. Duong, and Q.-T. Nguyen, "Developing a novel real-time indoor positioning system based on BLE beacons and smartphone sensors," *IEEE Sensors Journal*, vol. 21, no. 20, pp. 23055–23068, Oct. 2021, doi: 10.1109/JSEN.2021.3106019.
- [23] M. M. Rana, N. Halim, M. M. Rahamna, and A. Abdelhadi, "Position and velocity estimations of 2D-moving object using kalman filter: Literature review," in *2020 22nd International Conference on Advanced Communication Technology (ICACT)*, Feb. 2020, pp. 541–544. doi: 10.23919/ICACT48636.2020.9061241.
- [24] P. Srivastava, M. Bajaj, and A. S. Rana, "Overview of ESP8266 Wi-Fi module based smart irrigation system using IOT," in *2018 Fourth International Conference on Advances in Electrical, Electronics, Information, Communication and Bio-Informatics (AEEICB)*, Feb. 2018, pp. 1–5. doi: 10.1109/AEEICB.2018.8480949.
- [25] Y. Sangeetha, P. S. Sashank, C. V. Satyanarayana, and M. Geethika, "Development of weight system embedded with tracking system using Arduino UNO Rev3," in *2023 7th International Conference on Computing Methodologies and Communication (ICCMC)*, Feb. 2023, pp. 1411–1416. doi: 10.1109/ICCMC56507.2023.10084100.

BIOGRAPHIES OF AUTHORS






Ngoc-Son Duong    is currently pursuing the Ph.D. degree at the University of Engineering and Technology, Vietnam National University, Hanoi, Vietnam. His research interests include RF-based localization, and wireless communications. He can be contacted at email: sondn24@vnu.edu.vn.






Minh-Tuyen Vu    received B.S Degree at VNU University of Engineering and Technology in 2021. He is a member of the Telecommunication Systems Laboratory at VNU University of Engineering and Technology. His research interests include localization techniques and wireless communication. He can be contacted at email: 19020655@vnu.edu.vn.



Minh-Duc Nguyen    is a senior working toward a B.S. Degree at VNU University of Engineering and Technology. He is a member of the Telecommunication Systems Laboratory at VNU University of Engineering and Technology. His research interests include localization techniques and wireless communication. He can be contacted at email: 22029003@vnu.edu.vn.



Thai-Mai Dinh Thi    graduated from Post and Telecommunication Institute of Technology, Vietnam, in 2006. She received her M.Sc. degree from University of Paris Sud 11, France, in 2008, and her Ph.D. degree from VNU University of Engineering and Technology, Hanoi, Vietnam, in 2017. She is the Head of Department of Telecommunications Systems, Faculty of Electronics and Telecommunications, VNU University of Engineering and Technology, Hanoi, Vietnam. Currently, her research interests include 5G/6G mobile networks, wireless communications, localization techniques, and Security in SDN. She can be contacted at email: dttmai@vnu.edu.vn.